UNCLASSIFIED

AD 263 085

*Reproduced
by the*

ARMED SERVICES TECHNICAL INFORMATION AGENCY
ARLINGTON HALL STATION
ARLINGTON 12, VIRGINIA

UNCLASSIFIED

61-4-4 NOX

STUDIES OF A VENTILATED SUPERCAVITATING PROPELLER ON A TORPEDO TEST VEHICLE

Part 1. Performance Results

By

Paul C. Roberts
Underwater Ordnance Department

ABSTRACT. A torpedo test vehicle utilizing a ventilated supercavitating propeller was the subject of an experimental program carried out on the underwater cableway facility at Morris Dam. Vehicle runs, incorporating an 11-inch-diameter ventilated supercavitating propeller (DTMB 3819), showed the propulsive efficiency to average 79%. As gas was passed through the blade-ventilation holes in increasing amounts, the advance ratio progressively decreased by 10% but it could not be concluded that the efficiency was directly affected. Propeller performance data obtained with the actual test torpedo agreed with water-tunnel results reported by other laboratories.

U.S. NAVAL ORDNANCE TEST STATION

China Lake, California

21 February 1961

FOREWORD

In a field test program conducted by the Naval Ordnance Test Station, Pasadena, a ventilated supercavitating propeller, designed by the David Taylor Model Basin, was fitted to a high-performance torpedo and operated on an underwater cable facility. The program is significant in that data were accumulated under realistic operating conditions. Part 1 of this report describes the performance results; the acoustic data are presented in Part 2, classified Confidential.

The program reported was established by the Office of Naval Research in February 1959 and was carried out under ONR Task NR 062-224 entitled "Ventilated Propellers." The program was conducted during Fiscal Year 1959.

Review of this report for technical adequacy was performed by Andrew G. Fabula and T. G. Lang of this Station.

D. J. WILCOX, Head
Underwater Ordnance
Department

Released under
the authority of:

WM. B. McLEAN
Technical Director

CONTENTS

NOMENCLATURE

A_{in} Area of calibrated hub orifices, in^2

D Propeller diameter = 11 in.

e Propulsive efficiency = drag HP/shaft HP

g Acceleration of gravity = 32.2 ft/sec^2

H Absolute pressure at torpedo centerline minus cavity pressure in feet of water

J Advance ratio =V/nD

K_q Torque coefficient = $Q/\rho n^2 D^5$

K_t Thrust coefficient = $T/\rho n^2 D^4$

n Propeller revolution speed, rps

P_a Absolute pressure, psia

P_E Pressure at end of drive-shaft tube, psig

P_H Pressure inside propeller hub, psig

P_R Cavity pressure at 0.7 blade radius, psig

Q Measured torque, ft-lb

Q_{STP} Flow of venting gas, cfm, at standard conditions (15 psi and 70°F)

R Maximum propeller radius = 5.5 in.

R_Q Blade-filling ratio

T Thrust of propeller, lb = vehicle drag at constant velocity

T_a Absolute temperature, °F_{abs}

V Advance speed of torpedo, ft/sec

ρ Density of water = 1.94 slugs/cu ft

σ Cavitation number = $2gH/V^2$

INTRODUCTION

As torpedo speeds increase, it becomes more and more difficult to provide propeller-type thrust-producers that operate without cavitation with the resulting adverse effects on performance and the increase in noise and in blade erosion. Because it would be impossible to suppress such cavitation in the high-speed range (i. e. , typically above 50 knots), research programs have been launched to design and develop propellers that could be operated efficiently at high velocity with a fully developed cavity on the suction side of the blades. A supercavitating propeller (Fig. 1), having a blade cross section resembling a wedge rather than an airfoil, resulted (Ref. 1 to 4).

Supercavitating propellers have performed satisfactorily on surface vessels. However, the attainment of a fully developed blade cavity becomes difficult with underwater vehicles because of the high cavitation numbers encountered. In an effort to vary the cavity size at depth, a technique has been evolved in which permanent gas is injected into the low-pressure region in contact with the backs of the supercavitating propeller's blades. This process is called ventilation or forced ventilation. Although ventilated supercavitating propellers have displayed constant efficiencies over a wide range of ventilation rates, the lengthened gas-filled cavities that result have demonstrated a significant reduction in blade-surface erosion rates and noise generation.

The supercavitating propeller is a relatively new thrust-producer for surface-vessel operation. In the past, research and development have been conducted through towing-basin and water-tunnel experimentation under limited conditions. Although both these types of facility offer excellent photographic coverage and an almost unlimited adaptability to complete instrumentation, water or carriage velocities are relatively slow. Also, testing is limited to shallow depths in all towing basins and in some water tunnels. It was therefore apparent that a need existed for a test program that would extend present ventilated supercavitating propeller data to higher speeds and thrust loads, greater depths, and generally more realistic operating conditions for torpedo applications.

This report describes an experimental investigation conducted by the Naval Ordnance Test Station (NOTS) in which a ventilated supercavitating propeller was fitted to a high-speed research torpedo configuration. The vehicle was run captively on an underwater cableway facility so that the propeller's acoustic and performance characteristics

FIG. 1. Ventilated Supercavitating Propeller, Showing
Sharp Leading Edges, Thick Trailing Edges, Venting
Holes on Suction Side of Blading.

could be observed under varying ventilation rates. The results of the acoustic investigation are published separately in Part 2 of this report. This part describes the propeller's performance characteristics. Although a large quantity of the performance data essentially verifies results obtained by other laboratories through water-tunnel evaluations, much of the data expands upon that which is currently available. It is felt that the program is significant because the data were obtained directly with a high-speed torpedo. The program was of value to NOTS not so much for the performance information accumulated as for the experience gained in outfitting and operating an underwater vehicle with a ventilated supercavitating propeller.

METHODS OF INVESTIGATION

TEST FACILITY

A unique underwater cableway facility is operated by NOTS at the Morris Dam Torpedo Range, where a portion of a reservoir is bounded by two ridges of land approximately 3,500 feet apart. Anchor blocks were placed on both ridges to hold the ends of two 3/4-inch-diameter smooth-exterior steel cables. These cables, hanging parallel to each other in a catenary curve between the anchor blocks, resemble a long sweeping railroad track. The catenary extends to a maximum water depth of 66.5 feet and the total underwater trajectory is approximately 2,600 feet long. When a torpedo is to be captively operated on the cableway facility, the vehicle is equipped with four short airfoil struts with hardened steel guides or sliding shoes that attach to the cables.

The underwater cableway is an ideal facility for experimental programs such as the one described here. Because the vehicle travel is restricted to a predetermined path, there is no need for hydrodynamic control systems, and power-plant or thrust-producer evaluations are allowed to proceed at an accelerated rate. Also, since one of the cables is permanently magnetized at discrete intervals (every 5 feet), torpedo velocity can be accurately determined by sensing these magnetic markers with instrumentation inside the torpedo. The facility is also equipped with hydrophones placed at precise distances from the trajectory to record the torpedo's radiated noise. Because of the turbidity of the Morris Dam water, underwater photography of the cableway is seldom successful and was not attempted during this investigation.

TEST VEHICLE

The NOTS Research Torpedo test vehicle (Fig. 2 and 3) was used as a mobile dynamometer for evaluating the ventilated supercavitating propeller. This torpedo is powered by a single-wheel turbine operating on the decomposition products of

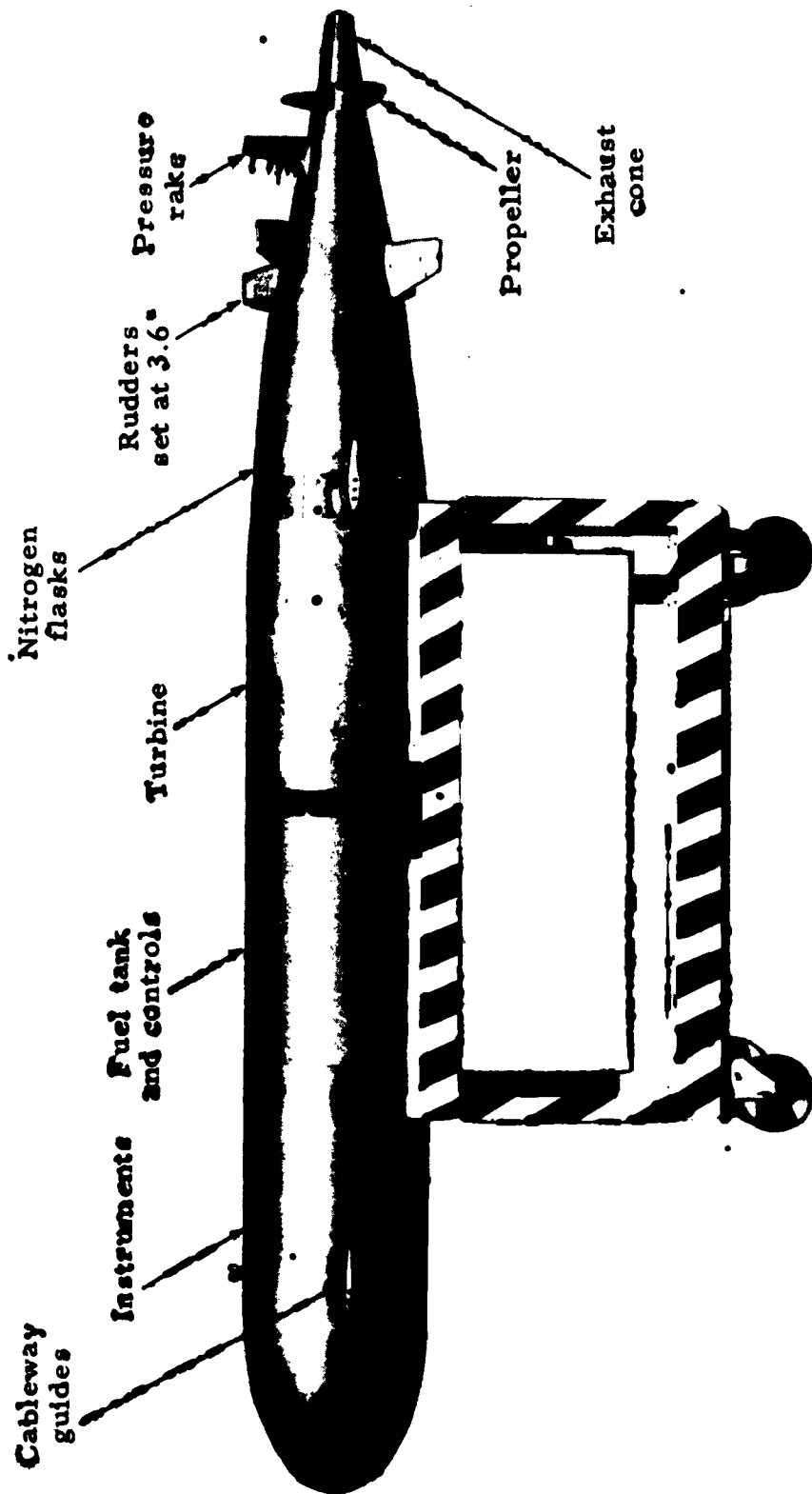FIG. 2. Test Vehicle on Cableway Prior to Launching.

FIG. 3. Internal Arrangement of Torpedo Configuration.

Cableway
guides

Instruments

Fuel tank
and controls

Turbine

Nitrogen
flasks

Rudders
set at 3.6°

Pressure
rake

Propeller

Exhaust
cone

hydrogen peroxide. The propeller shaft is driven directly at turbine speed. The vehicle is well suited for testing any new propeller design since the direct connection between the turbine and propeller allows a wide range of power to be delivered over a wide range of rotative speed. Only the pressure of the decomposing hydrogen peroxide monopropellant need be changed for operation at the power-rpm condition desired. Also, a sufficient quantity of turbine exhaust gas is available to fill the blade cavities of a ventilated supercavitating propeller.

Figure 3 indicates the arrangement of the test vehicle's internal components. The torpedo is 15 inches in diameter, 120 inches long (with exhaust cone), and weighs 590 pounds in air. The nose section contains the instrumentation package used for recording all performance data. The next section consists of the valving, regulator, and tank for the 90% hydrogen peroxide fuel system. Just aft of the torpedo midpoint is the 12-inch-diameter tangential-flow Terry turbine. Figure 4, illustrating the turbine's internal configuration, shows the four nozzles with separate reversing chambers. The torpedo afterbody houses nitrogen flasks that are incorporated in the fuel-feed pressurization system. The afterbody is also fitted with four rudders set at a 3.6° deflection for counteracting the torque of the single propeller.
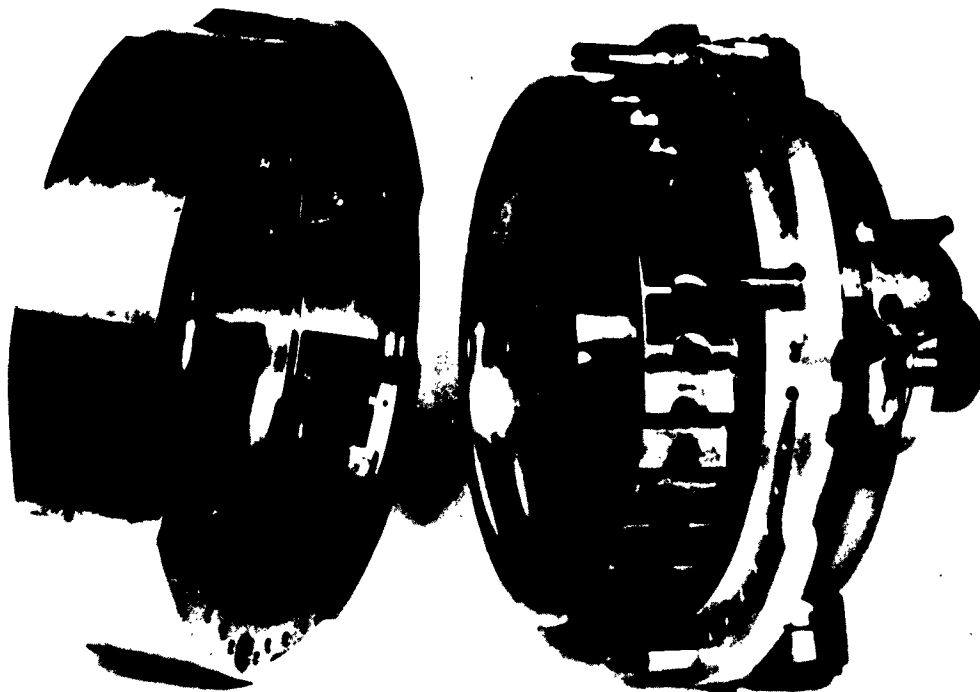

FIG. 4. Tangential-Flow Turbine Incorporating Four Nozzles and Reversing Chambers.

The gas driving the turbine is composed of 29.2% oxygen and 70.8% steam by volume. A portion of this gas was used to ventilate the propeller and the remainder was allowed to pass through the exhaust cone approximately 6 inches aft of the propeller plane. Figure 5 illustrates the system used to control and measure the quantity of venting gas. The calibrated hub orifices (of various sizes) were changed between runs to allow the hub chamber pressure to vary and thus vary the flow of gas through the root and blade holes. The pressure in the exhaust system could be increased by placing plugs in the exhaust cone flow-restrictor. This forced more gas to flow through the root and blade holes.

PROPELLER

The 11-inch-diameter ventilated supercavitating propeller[1] (TMB 3819) was designed by the David Taylor Model Basin for a forward speed of 65 knots, a rotative speed of 7,500 rpm, a thrust of 1,341 pounds, and a propulsive efficiency of 70%. From these values, the advance ratio J can be computed as 0.96, the thrust coefficient K_t as 0.0627, the torque coefficient K_q as 0.0136, and the shaft horse-power requirement as 382.

Figure 6 shows the root and blade gas ventilation holes plus a small hole at the 0.7 radius point for sensing blade cavity pressure.

INSTRUMENTATION

All performance data were recorded with instruments inside the test vehicle. The heart of this instrumentation system was a Midwest 14-channel galvanometer-type oscillograph. Recorded on the oscillograph were the various functions required to monitor the performance or environment of the vehicle and thrust producer, the operation of the power plant, and the gas-flow quantity utilized for propeller ventilation. The decomposition-chamber pressure, exhaust pressure, and propeller hub and cavity pressures were sensed with strain-gage-type transducers. Gas-exhaust temperature was monitored by thermocouples. Rotative speed of the propeller shaft was digitally determined by means of a magnet and coil pick-up. Torque measurements were obtained from strain-gage-instrumented flexure beams on which the turbine case was mounted. Data on the forward speed of the torpedo was acquired from the magnetic cableway markers, which also provided an accurate determination of the vehicle's position along the underwater trajectory and thus a continuous indication of the operating depth.
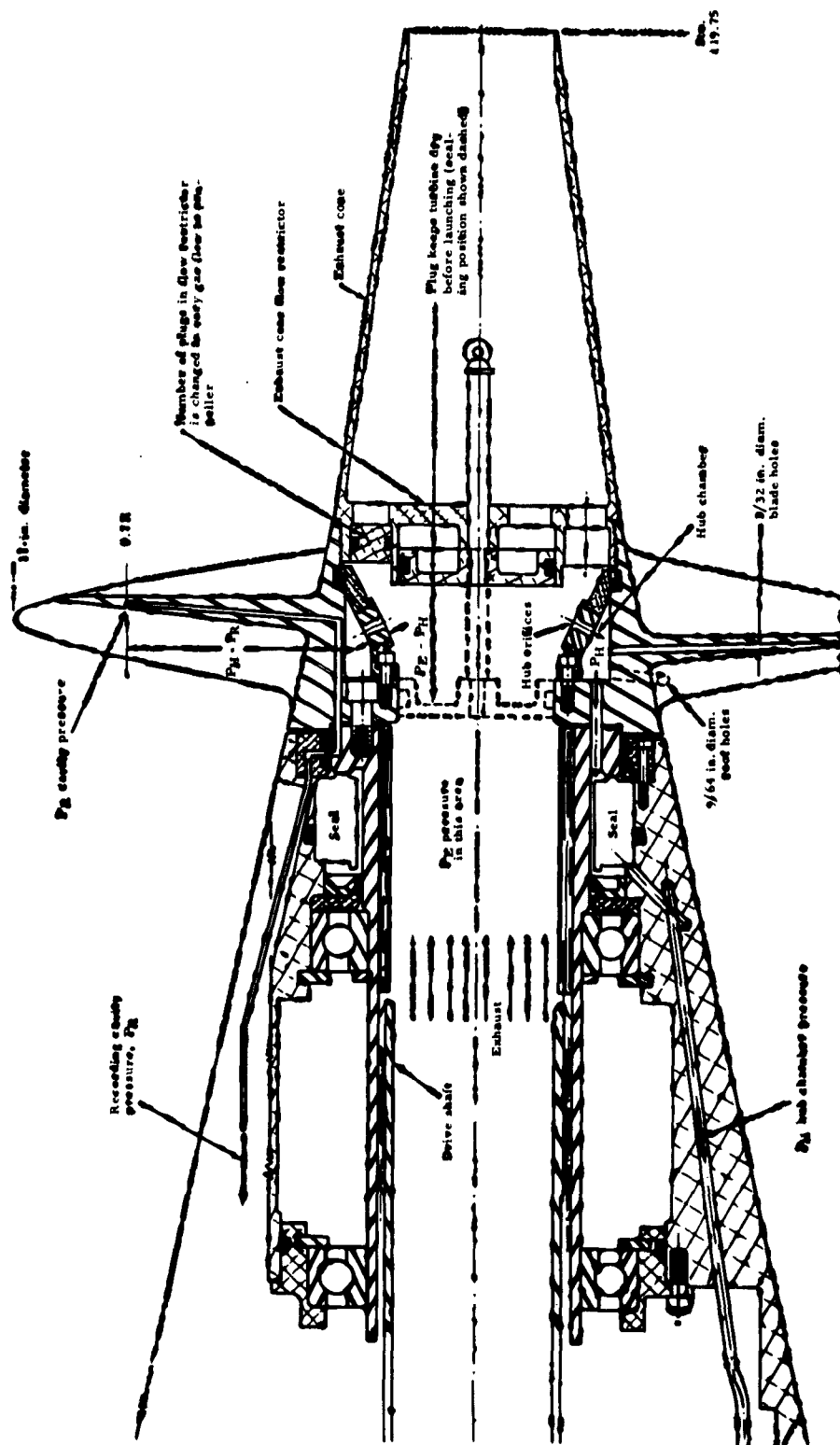
---

[1] NOTS SK 465498.

FIG. 5. Propeller Venting System.

FIG. 6. Propeller Showing Blade Venting Hole and
Cavity-Pressure Sensing Hole.

In order to obtain a velocity profile of the water flowing into the
propeller plane, the afterbody of the vehicle was fitted with a pressure-
sensing rake (Fig. 3 and 7). Although velocity-profile information is
not required for determining performance levels in the field, it is use-
ful to the propeller designer for comparison with the original inlet
velocity assumptions. Results of the pressure-rake measurements
are given in Appendix A.

Calibration of the instrumentation system indicated an over-all
accuracy of ±2% for all transducers except the torque cell, which pro-
duced variations of ±9%. Galvanometer response time was approxi-
mately 0.2 second.

RANGE PROCEDURES

Thirteen cableway runs with the TMB 3819 ventilated supercavitat-
ing propeller were made. Just prior to launching, the vehicle was
attached to the cableway by bolting the four guide shoes to the airfoil
struts (Fig. 2). The torpedo was then pushed down the cableway to the
starting depth (5 feet for all tests except the two final high-speed runs
when the starting depth was 15 feet), and an external lanyard was
pulled to actuate the run programmer. This cam-actuated switching
device provided the necessary time sequencing for warming up the
instrumentation, bringing the oscillograph up to speed, and starting

FIG. 7. Pressure Rake Measures Water Velocity Profile at
Propeller Plane.

the power plant. At the end of each run, all power was shut off and the
torpedo came to a complete stop just past the middle of the cableway
trajectory. A recovery boat towed a separate cableway sweep back-
wards along the cables to return the test vehicle to the launching barge.
The oscillograph magazine was removed after each run for immediate
processing of the record.

The information obtained by the oscillograph was plotted on indi-
vidual run records. A portion of the reduced data from a typical run
is shown in Fig. 8. It can be seen that as the vehicle reaches greater
depths in the lake, the back pressure on the turbine reduces the speed
and also causes a fall-off of torque, rotative speed, and shaft horse-
power.

DATA REDUCTION TECHNIQUES

Gas-Flow Rates

The gas-flow rates used for propeller ventilation were determined
with the changeable hub orifices shown in Fig. 5. The orifices were
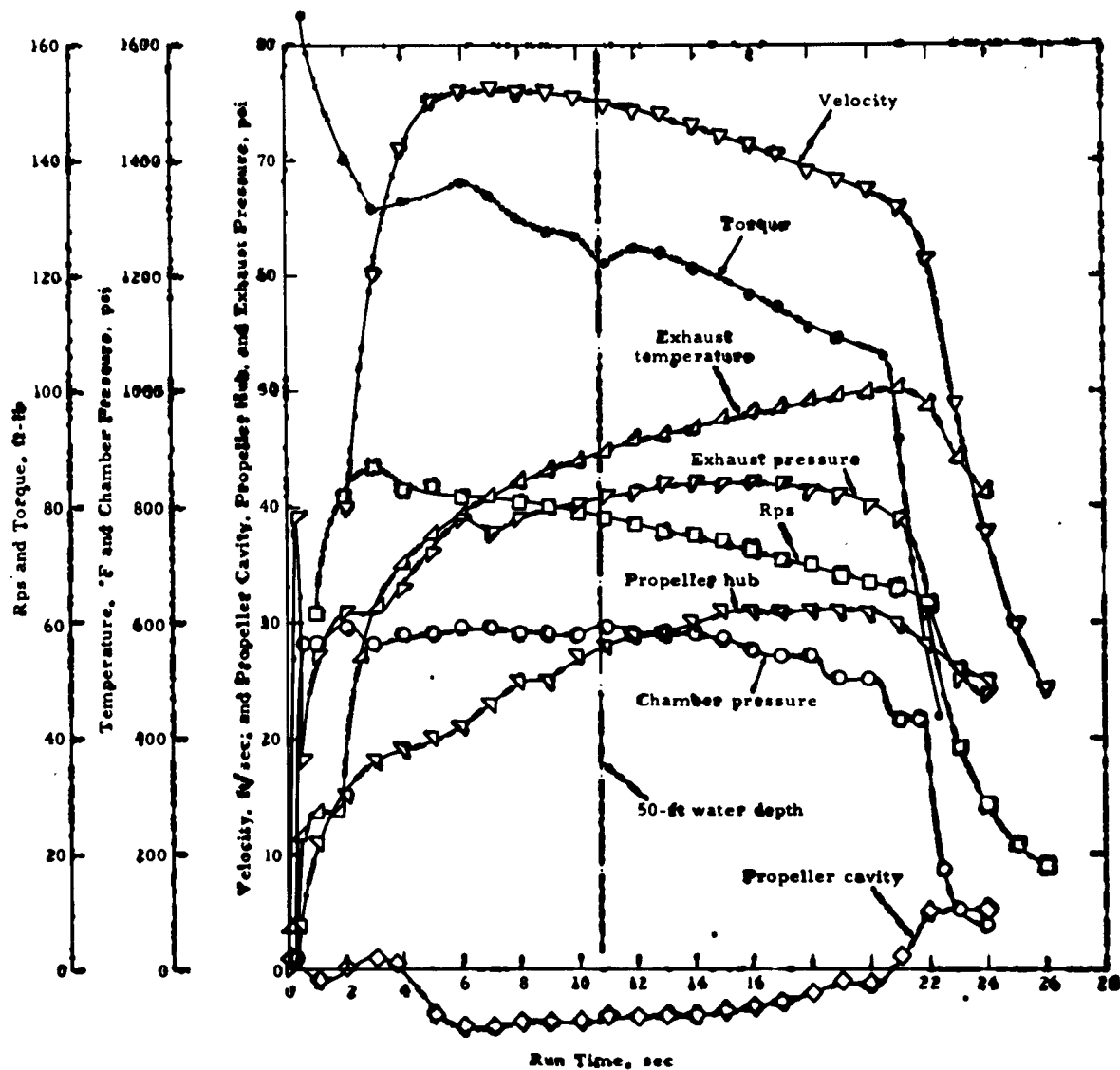
FIG. 8. Typical Plot of Recorded Data, J = 1.047.

calibrated in the laboratory, and the following empirical relationship resulted for total gas flow:

$$Q_{STP} = 753\, A_{in} \sqrt{\frac{(P_E - P_H)P_a}{T_a}}$$

These quantities are defined in the Nomenclature and the pressures are also indicated in Fig. 5. It should be noted that P_E was determined by calculating the pressure drop down the drive-shaft tube. The turbine case and exhaust pressures, as recorded by the internal instrumentation on certain runs, provided the means of calibrating this pressure drop.

All steam contained in the hot exhaust products was assumed to condense upon entry into the propeller-blade cavities. Only the oxygen, 29.2% by volume, was considered as a permanent cavity-filling gas. The modified hub-orifice relationship is

$$Q_{STP} = \frac{29.2}{100}\,(753)A_{in} \sqrt{\frac{(P_E - P_H)P_a}{T_a}} = 220\, A_{in} \sqrt{\frac{(P_E - P_H)P_a}{T_a}}$$

Laboratory calibrations were typically consistent to within ±6%. However, when the flow rate was low, P_E and P_H were nearly equal and a 50% error in the pressure difference was possible. This condition was experienced in Runs No. 2, 3, and 7. Nevertheless, for the small amounts of gas ventilation for those runs, no significant change in the conclusions would be experienced even if those ventilation rates were changed by a factor of two.

The propeller ventilation holes were also used as calibrated orifices for those runs in which the blade cavity pressure was recorded. The pressure drop employed in the associated calibration equation, $P_H - P_R$, is indicated in Fig. 5. The blade-venting holes provided back-up instrumentation with which to check the ventilation rates as computed from the hub orifice data.

Propulsive Efficiency

The turbine or propeller rotative speed was combined with the recorded torque to yield shaft horsepower as follows:

$$SHP = \frac{2\pi Q n}{550}$$

Propulsive efficiency was obtained by dividing the drag horsepower by the shaft horsepower. Drag horsepower is defined as

$$DHP = \frac{\text{vehicle drag} \times \text{vehicle velocity}}{550}$$

The test vehicle's bare-body drag was determined in the California
Institute of Technology low-speed wind tunnel. To this bare-body
value, a 5% increase was added for the fin area with deflected rudders.
A 20% increase was also added to account for the effect of the propel-
ler disturbance on the bare-afterbody pressure distribution (thrust
deduction), the airfoil-strut drag, and the shoe friction on the cables.[2]
The cubic relationship between drag power and vehicle velocity was
applied to the wind-tunnel evaluation point (data taken at 40 knots). The
resulting curve of drag power versus velocity is shown in Fig. 9. The
propeller's thrust and torque coefficients K_T and K_Q were computed
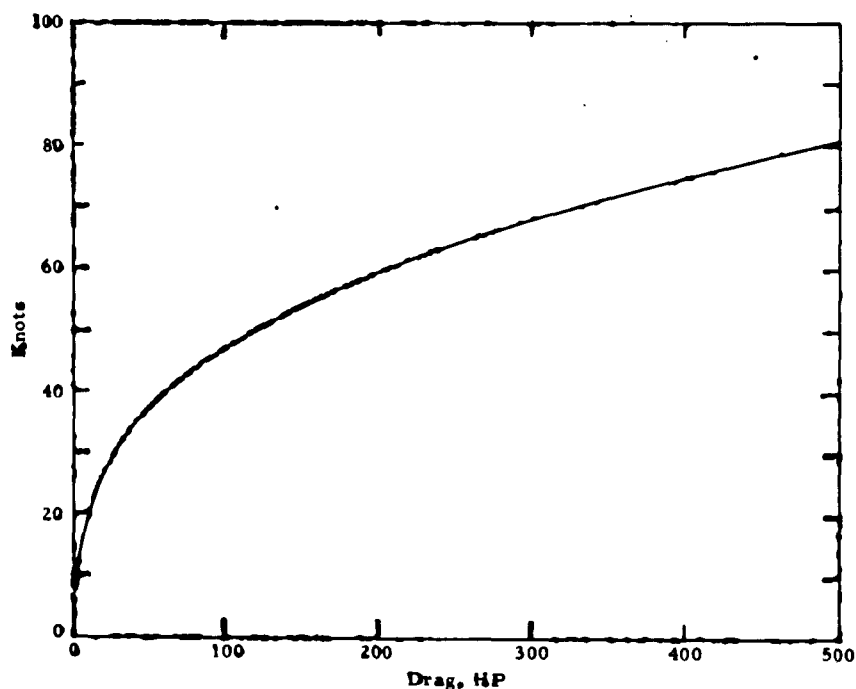from these drag-curve data and the recorded torque, respectively.

FIG. 9. Drag Horsepower as Calculated for
Design Evaluation and Data Reduction.

---

[2] Previous shoe-drag measurements established the coefficient of
friction at 0.1, while the shoe load for the vehicle was approximately
80 pounds. This increased the drag by 8 pounds, which is small com-
pared to the total drag of approximately 490 pounds at 40 knots.

Blade-Cavity Pressure and Cavitation Number

The measurement of propeller blade-cavity pressure was started on Run No. 7. This cavity pressure was sensed through a small orifice located at the 0.7 radius point (Fig. 6). The pressure was then transmitted through a small passage to the internal transducer. As shown in Fig. 5, this passage is bounded in one area by two O-ring rubbing seals. Since the rubbing velocity was as high as 6,000 fpm, lubrication was a definite problem. Graphite grease was used on Run No. 7, but it was found that the thick grease plugged the small passageways. For the following six runs, a lubricant consisting of 75% Dow Corning 550 silicon oil and 25% rust inhibitor was employed on the O-rings and the rotating hub was lightly coated with electrofilm spray. This combination proved successful and five runs[3] yielded cavity-pressure records suitable for engineering analysis.

The recorded blade-cavity pressures were used to compute the cavitation numbers as

$$\sigma = \frac{2gH}{V^2}$$

where the quantity H represents the absolute pressure head at the torpedo center line minus the blade-cavity pressure (in feet of water).

Blade-Filling Ratio

A new relationship, entitled the blade-filling ratio R_Q, introduced here, should prove a useful parameter for comparing different propeller designs and determining the gas-ventilation quantities for new propeller designs. The blade-filling ratio is defined as the quantity of gas (standard temperature and pressure, STP) per unit time employed for propeller ventilation divided by the volume generated per unit time by the blade trailing-edge thicknesses as they move through the water. For each trailing edge of the propeller under evaluation, the tip was 1/32 inch thick and the root was 13/32 inch thick. Each such area follows a helical path to evolve one third of the total volume generated by the three-bladed propeller. This volume is calculated in Appendix B. Since the total recorded volume of ventilating gas is compared to the total volume generated by the propeller's trailing edge, it is seen that the blade-filling ratio indicates that portion of a characteristic cavity being filled by venting gas.

---

[3] During Run No. 9, a small strip of O-ring was sheared off and plugged the pressure line.

Advance Ratio

In several of the performance charts to follow, the advance ratio J is used as either the dependent or the independent variable. The advance ratio is defined as

$$J = \frac{V}{nD}$$

It is seen that the advance ratio represents the forward movement of the vehicle, expressed in propeller diameters, for each revolution of the propeller. The advance ratio, thrust coefficient, torque coefficient, and propulsive efficiency are related by the following expression:

$$J = 2\pi e \frac{K_Q}{K_T}$$

DESCRIPTION OF RUNS

Results of 12 of the 13 cableway runs are tabulated[3] in Table 1. Performance data are listed for that instant when the vehicle passed the 50-foot-depth level on the cableway.

Table 1 shows that the gas-ventilation flow rates were continuously increased for the first six runs. The next two tests (No. 7 and 8) were repeats of earlier runs (Run No. 3 and 6). For Run No. 9, the propeller-blade and root-ventilation holes were purposely plugged and the exhaust cone (with its internal flow-restrictor) was removed from the vehicle. Thus, exhaust gases left the vehicle through the hub which was only 3/8 inch to the rear of the propeller's trailing edges. This was done to determine whether ventilation could be accomplished without direct cavity injection. Runs No. 10 and 11 were concerned with exhausting turbine gases at the side of the vehicle, and none through the blade holes. The ventilation came only from bubbles in the water and was estimated as less than 1 cfm. Runs No. 12 and 13 were final high-speed tests employing large quantities of ventilation gas.

The remainder of the performance data in Table 1 were obtained by the instrumentation and techniques described above. Unfortunately, the torque cell was overloaded during Runs No. 12 and 13 so that shaft horsepower and propulsion efficiency could not be computed.

---

[3] Run No. 4 was unsatisfactory and is not shown.

TABLE 1. Comparative Test Data Tabulated for Vehicle at 50-Foot Depth

Run No. 4, unsatisfactory, is not shown.

Parameter	Run No.										High-Speed Run No.	
	1	2	3	5	6	7a	8b	9	10	11	12	13
Speed, knots	42.8	42.9	42.9	45.8	41.5	42.6	40.3	42.7	44.9	45.1	59.3	56.3
RPM	4410	4430	4500	5000	4800	4500	4650	4500	4740	4800	6600	6300
Advance ratio $J = V/nD$	1.08	1.07	1.05	1.02	0.96	1.05	0.97	1.05	1.04	1.04	1.00	0.99
Gas vented through blades, cfm	0	0.7	3	20	50	3	50	0 (No exhaust cone)	Estimated as less than 1 (Side exhaust)c		40	50
Propeller cavity pressure at 0.7R, pstg	Cavity pressure not recorded					Transducer line plugged	+5	Transducer line plugged	-4.5	-5.0	+4.5	+4.0
Shaft horsepower	98	91	99	114	82	100	68	83	117	118	Torque cell failed on Runs 12 and 13	
Propulsive efficiency	0.77	0.83	0.74	0.80	0.79	0.74	0.88	0.84	0.74	0.75		

a Repeat of Run No. 3.
b Repeat of Run No. 6.
c See page 15.

EXPERIMENTAL RESULTS

VENTILATION VERSUS ADVANCE RATIO

As can be seen in Table 1, the performance parameter that varied most consistently with ventilation flow rate was the advance ratio J. As the ventilation rate was increased from 0 to 50 cfm during the first six runs, the advance ratio steadily decreased from 1.08 to 0.96 (for the 50-foot depth). It is clear that this trend is real because the advance ratio was very accurately established from the digitally determined vehicle velocity and propeller-shaft speed.

Judging from the high advance ratio that resulted during Run No. 9, it was concluded that the indirect ventilation that was attempted by exhausting gas close to the trailing edges of the blade was not totally successful. The resulting advance ratio of 1.05 corresponds to that obtained during Run No. 3 when the direct ventilation flow rate was 3 cfm. Conceivably, a much greater effect might have been produced if the hub had been cut back closer to the trailing edges of the blade.

During any individual run, the slope of the cableway and the resultant ambient pressure increase affected many of the performance parameters, including the advance ratio. The volume of venting gas calculated for standard temperature and pressure conditions, Q_{STP}, remained relatively constant for each run. However, as the cavity pressure increased with depth, the actual volume of gas supplied to the propeller cavity would decrease by approximately 25%. This volume change, along with simultaneous variations in shaft speed and vehicle velocity, influenced the advance ratio. The resulting effect is plotted in Fig. 10.

BLADE-FILLING RATIO VERSUS ADVANCE RATIO

Just as the advance ratio varied consistently with gas-ventilation flow rate, it automatically follows that it varied consistently with the blade-filling ratio. Figure 11 shows the blade-filling ratio plotted versus advance ratio for all tests in which the ventilation flow rate was known. The solid-line curve of Fig. 11 shows this relationship when it is computed with ventilation flow rates based on standard temperature and pressure conditions. If these ventilation rates were calculated for actual cavity pressures, a maximum correction in R_Q of approximately 25% would be effected for any given advance ratio. A portion of the corrected curve, based upon three of the runs for which the cavity pressure was recorded, is shown as a dashed line in Fig. 11. It is seen that the relationship between R_Q and J is quite linear for gas-ventilation rates in excess of approximately 3 cfm and that a 10% reduction in advance ratio took place when the hypothetical helical cavity was approximately one quarter filled with permanent gas.
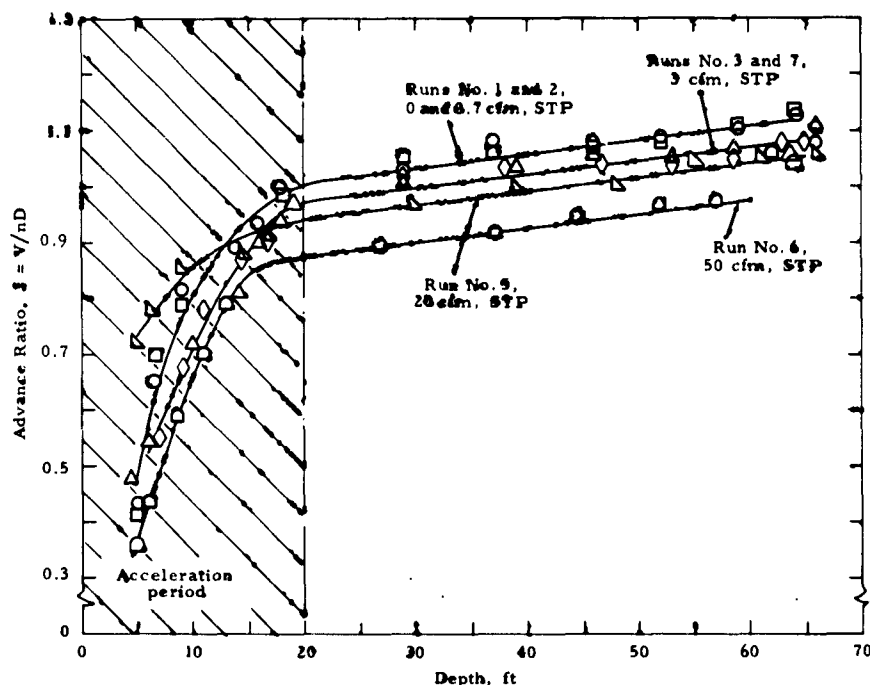
FIG. 10. Variation of Advance Ratio With Depth and
Varying Amounts of Venting Gas.

CAVITY PRESSURE RELATIONSHIPS

The blade-cavity pressure was successfully recorded for five runs
(No.8, 10, 11, 12, and 13). The resulting data are plotted versus op-
erating depth in Fig. 12. A convenient display is achieved by dimen-
sioning the cavity pressure in feet of water along with the ambient
depth, atmospheric, and saturated water-vapor pressures on the same
graph. Figure 12 shows that the blade-cavity pressure is approximately
proportional to the gas-ventilation flow rate. Cavity pressure was well
above the vapor pressure of 70°F water even at the minimum ventila-
tion rate of 1 cfm. It is unfortunate that blade-cavity pressure was
not recorded for Run No. 1 to verify supercavitating operation under
zero ventilation.

Cavitation numbers were computed for the five runs listed above,
and three representative curves of this parameter are also plotted
versus operating depth in Fig. 12. The minimum cavitation number,
$\sigma \approx 0.28$ at 50-foot depth, occurred on Run No. 12, which gave the
highest speed.

COMBINED PERFORMANCE CHARACTERISTICS

In presenting test results of supercavitating propeller evaluation
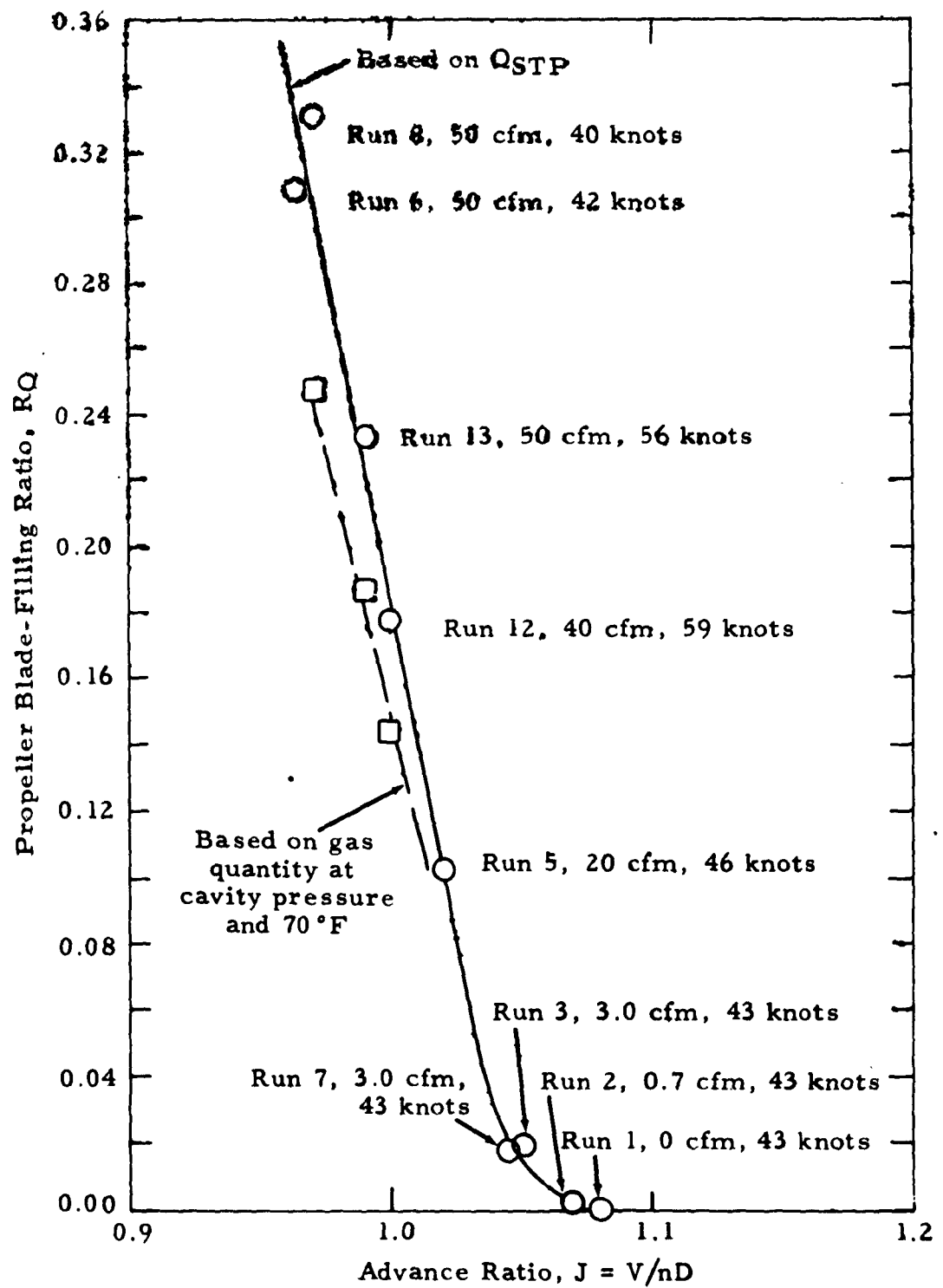programs, it has been customary to plot the propeller's propulsive

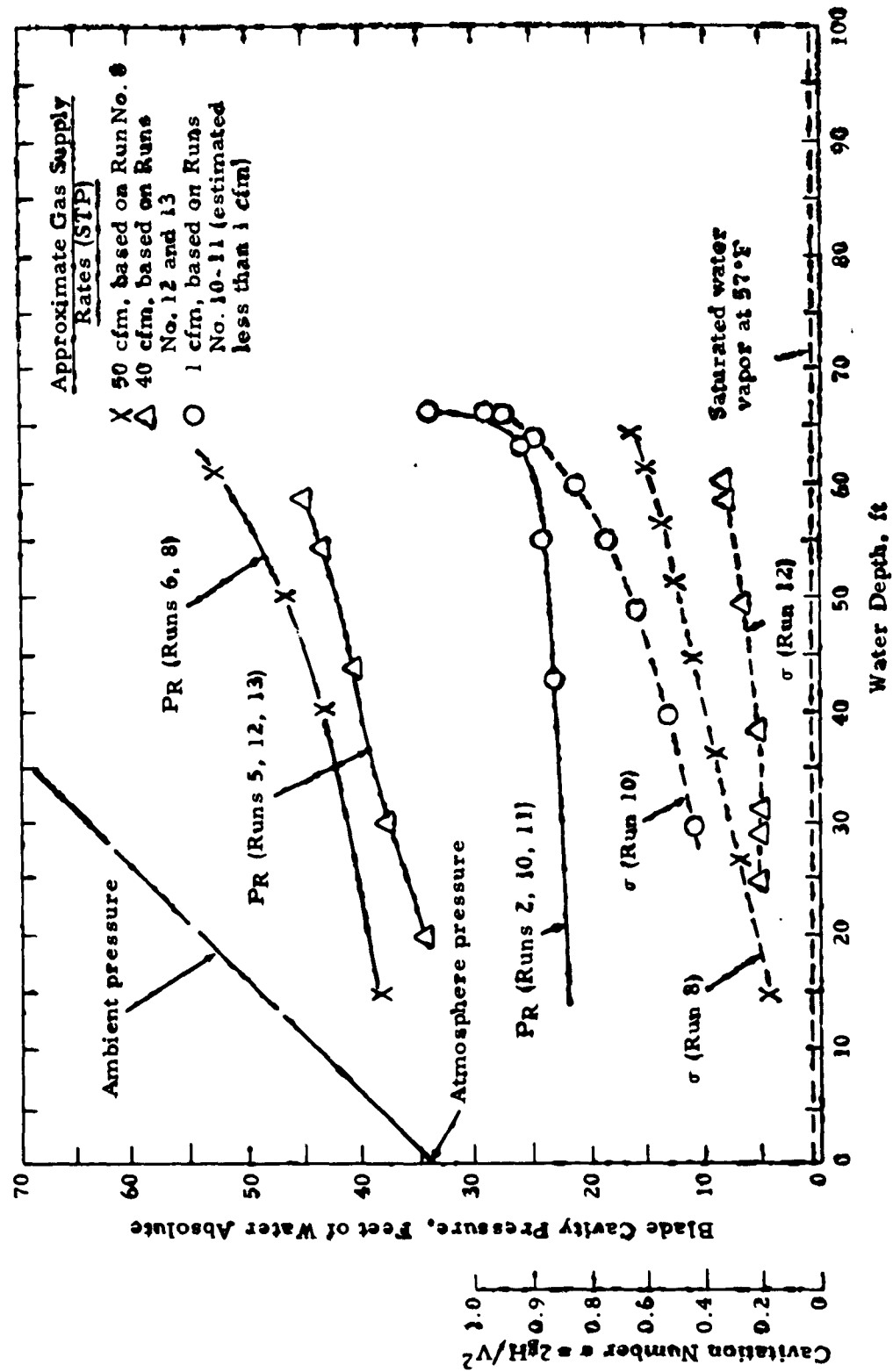FIG. 11. Blade-Filling Ratio Versus Advance Ratio at
50-Foot Depth.

FIG. 12. Cavity Pressure and Cavitation Number Versus Depth.

efficiency, thrust coefficient, and torque coefficient as functions of advance ratio on the same graph. When sufficient data are available, it has also been customary to present a family of curves for different cavitation numbers (Ref. 1 and 4).

Figure 13 shows a graphical display of this type (i.e., e, K_t, K_q versus J). Individual curves are shown for Runs No. 1, 3, 5, and 6 wherein the ventilation flow rates were 0, 3, 20, and 50 cfm, respectively. The dashed-line segment of each curve represents that initial portion of the run when the vehicle was accelerating to nominal speed.

Figure 13 shows no consistent trend in the propulsive efficiency as the advance ratio changes. However, because the ventilation rate progressively increased on Runs No. 1, 3, 5, and 6, there seems to be an increase in efficiency with increasing gas supply. However, the torque cell inaccuracy was ±9%. Its calibration varied not only before and after runs, but there were inconsistent rates of change of torque during some of the runs. Thus, the large torque inaccuracy makes it difficult to justify the suggested trend due to ventilation rate changes. By analyzing all data, an average value of propulsive efficiency of 79% was obtained, in contrast to the TMB design value of 70%.

Figure 13 shows that both the thrust and torque coefficients increased in a linear fashion with increasing advance ratio during any individual run and still assumed their approximate design values at the design advance ratio. There is a definite trend in the behavior of the torque coefficient as the ventilation rate was increased steadily from Run No. 1 to Run No. 6 (i.e., K_q decreases as ventilation rate increases at a fixed advance ratio). A similar trend is present but less apparent in the behavior of the thrust coefficient.

It is again stressed that the curves of Fig. 13 represent the performance characteristics noted during individual runs. Many system parameters vary during the course of a run because of the progressively changing depth along the cableway catenary. Earlier illustrations in this report showed the resulting variations in velocity, turbine speed and torque, ventilation control pressures, advance ratio, cavity pressure, and cavitation number. This situation complicates any attempt to isolate independent variables on which to base performance graphs. Nevertheless, because the cavitation number has been typically used as a performance-controlling criterion in previous supercavitating propeller investigations, it is worth while to review the possible effect of this parameter on the present results.

Since, as shown in Fig. 10, the advance ratio continuously increased during any individual test, it can be seen that run time would continuously increase to the right in Fig. 13. Also, as seen in Fig. 12, the cavitation number typically increased with run time because of the combined effect of increasing depth and decreasing velocity. Thus, for any curve of Fig. 13, the cavitation number
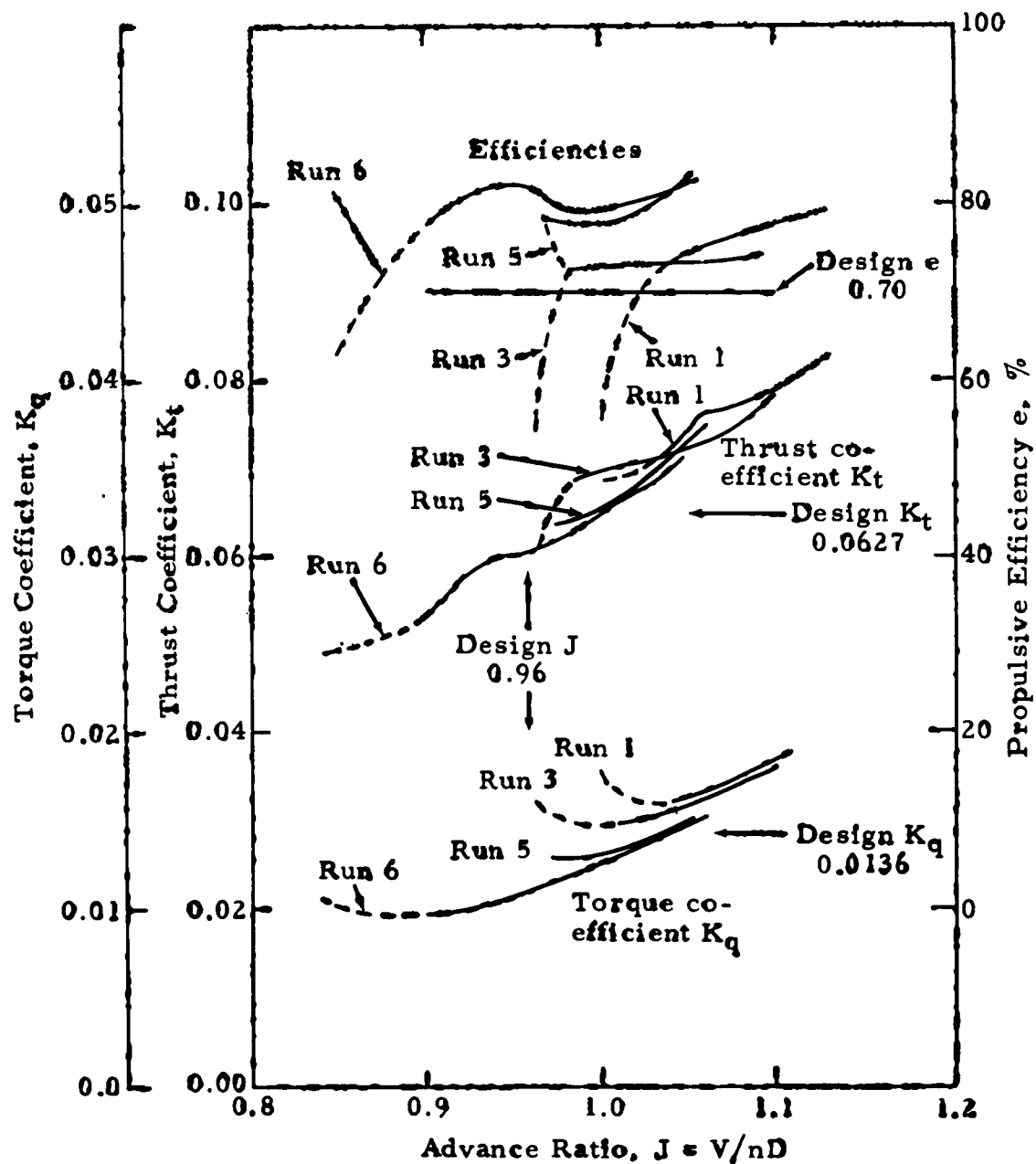
FIG. 13. Propulsive Efficiency, Torque and Thrust Coefficients.
(Dashed portion of curve indicates acceleration period.)

increases with advance ratio. Whereas past experimenters (Ref. 1 and 4) have shown the thrust and torque coefficients to decrease with increasing advance ratio (opposite to the effect shown in Fig. 13), they have also shown these coefficients to increase with cavitation number at any fixed advance ratio. Since the curves of Fig.13 represent increasing cavitation numbers as they proceed to increasing advance ratios, this combined effect would tend to explain why these curves slope in a direction opposite to those resulting from past experimentation. Because of the lack of sufficient cavity pressure measurements, no attempt was made to quantitatively isolate this effect.

VENTILATION LIMITATIONS

With power-plant exhaust gases being used for propeller ventilation, the fixed size of the blade-venting holes was an important limiting factor. With a fixed hole size, the turbine back-pressure had to be raised in order to increase the volume of venting gas. This reduced the turbine nozzle pressure ratio, with the result that power output was also reduced.

DTMB requested that the high-speed runs be made with the maximum gas-ventilation flow rate in an attempt to obtain an advance ratio near the design value of 0.96. However, increasing the gas-flow rate from 40 to 50 cfm (Runs No. 12 and 13, respectively) only changed the advance ratio from 1.00 to 0.99 at a 50-foot depth. Because of the higher hub pressures required, the speed was also reduced from 59.3 to 56.3 knots, representing a loss of approximately 30 horsepower. Further increase in the turbine back-pressure was not attempted since the exhaust tubing was originally designed for only 100 psi. In future designs, the propeller-hole sizes must be considered for their effect on the over-all performance of the power plant.

CONCLUSIONS

The results of the program prove that the ventilated supercavitating propeller can be successfully used on a high-performance underwater torpedo with the inherent performance advantages of a high allowable shaft speed, an excellent propulsive efficiency, and a high vehicle velocity without need for cavitation suppression at the thrust-producer.

The experimental field data, although not as precisely controlled as in equivalent laboratory programs, were nevertheless obtained under more realistic conditions of velocity, power level, and operating depth. These data showed that the ventilated supercavitating propeller was operated at or near its design conditions insofar as advance ratio, thrust coefficient, and torque coefficient were concerned.

Because of the problem in matching the propeller's ventilation requirement at high speed to the exhaust-gas supply limitations, only

about 90% of the design speed was ultimately attained. Nevertheless, the propeller displayed an efficiency well beyond its design value of 70% throughout all phases of the investigation.

It can be stated that the ventilated supercavitating propeller can be effectively employed with a high-speed torpedo as long as a sufficient quantity of gas at suitable injection pressure is available for ventilation.

Appendix A
BOUNDARY-LAYER VELOCITIES AT
PROPELLER PLANE

Before actually computing the blade-setting angles and blade-lift distribution, the propeller designer must determine the water-velocity profile at the inlet to the propeller plane. This profile is analytically resolved after a particular vehicle configuration and advance velocity are assumed. The hydrodynamicist is interested in knowing the actual velocity distribution that results in the field once the propeller is placed in operation, in order to compare it with his initial design calculations. To secure this information, a pressure-sensing rake was fitted to the vehicle (Fig. 7 and 14). The resulting data are shown in Fig. 14 as a plot of dimensionless velocity versus position on the rake. The dimensionless quantity is defined as "local velocity" divided by "forward velocity." Figure 14 is plotted as a large-scale drawing showing the rake position in relation to the propeller. The body static pressure, as sensed at Point F of Fig. 14, was 1 to 2 psi greater than depth pressure at a 43-knot advance velocity.
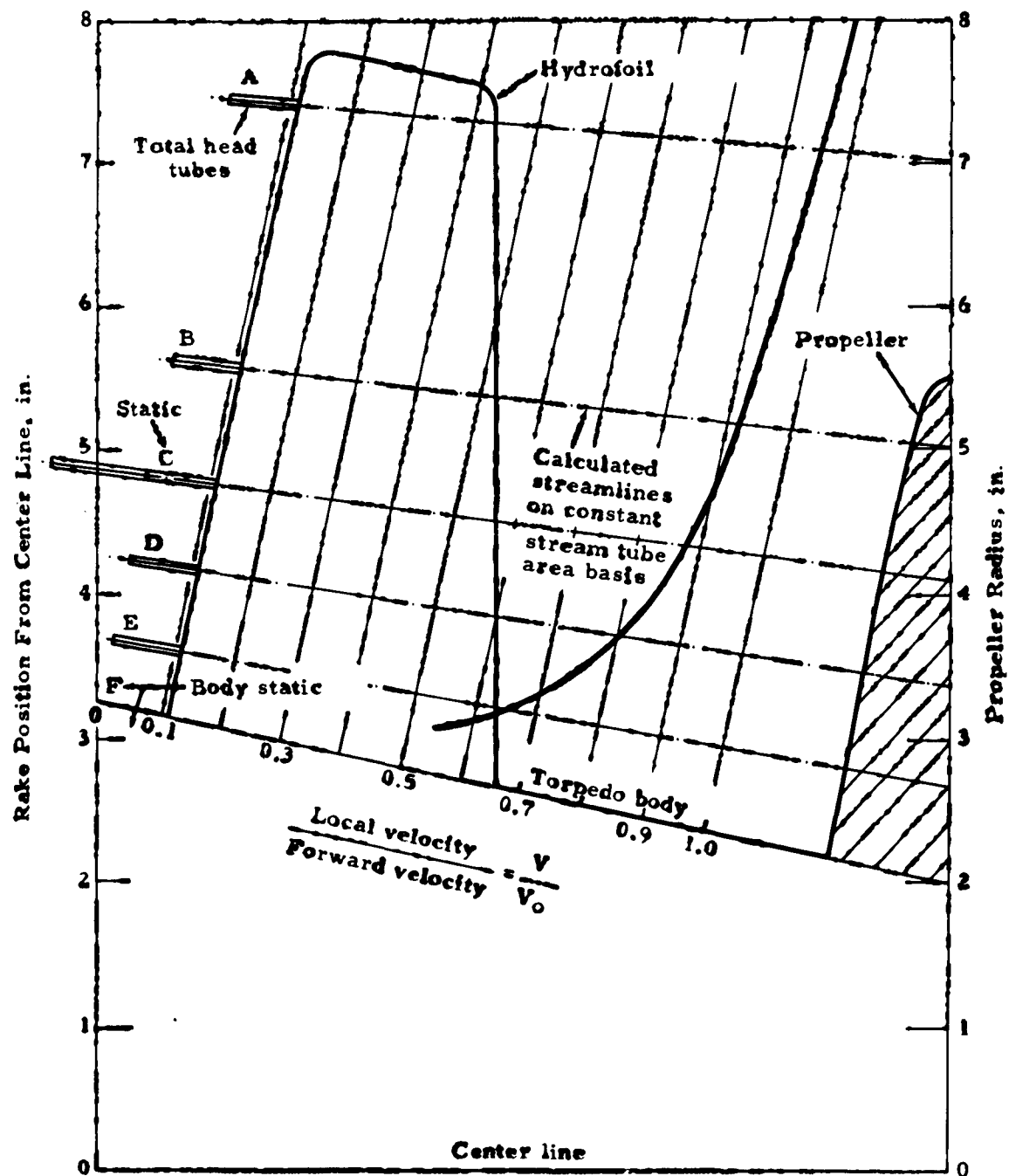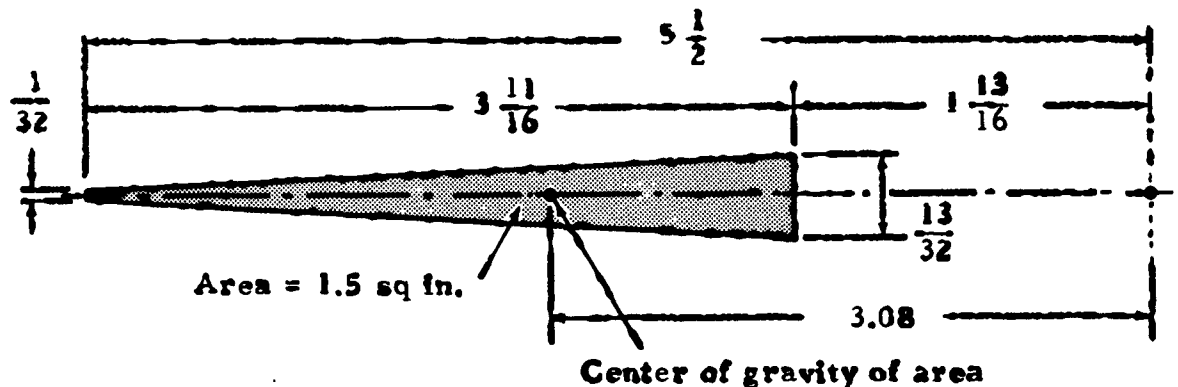
FIG. 14. Boundary-Layer Velocities.

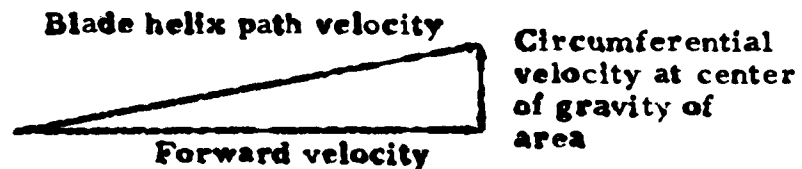## Appendix B

CALCULATION OF CHARACTERISTIC CAVITY VOLUME

As the propeller blades turn through the water, the thick trailing edges move in a helical path and generate a characteristic volume, Q_c. This volume is calculated as follows:

Area = 1.5 sq in.

Center of gravity of area

The sketch shows the dimensions of each blade cross section. The total blade cross section area is

$$1.5 \times 3 = 4.5 \text{ sq in.} = 0.0312 \text{ sq ft}$$

According to the following velocity diagram,

Blade helix path velocity

Circumferential velocity at center of gravity of area

Forward velocity

the helix velocity is

$$\sqrt{\left(\pi \times rps \times \frac{6.16}{12}\right)^2 + V^2} \text{ ft/sec}$$

The characteristic volume generated by three blades is

$$Q_c = \text{area} \times \text{helix velocity}$$

$$Q_c = 0.0312 \sqrt{\left(\pi n \frac{6.16}{12}\right)^2 + V^2} \quad \text{cu ft/sec}$$

and the blade-filling ratio, R_Q, is

$$R_Q = \frac{Q_{STP}}{Q_c}$$

REFERENCES

1. Tachmindji, A. S., and W. B. Morgan. "The Design and Estimated Performance of a Series of Supercavitating Propellers," Second Symposium on Naval Hydrodynamics, Proceedings. Office of Naval Research, Washington (29 August 1958).

2. Morgan, W. B. "Performance of a Ventilated Propeller," presented at American Towing Tank Conference, Berkeley, Calif. (31 August 1959).

3. David Taylor Model Basin. TMB 3-Bladed Supercavitating Propeller Series, by E. B. Caster. Washington, DTMB, August 1959. (DTMB Hydrodynamics Laboratory Research and Development Report 1245.)

4. ———. The Design and Performance of Supercavitating Propellers, by A. J. Tachmindji, W. B. Morgan, M. L. Miller, and R. Hecker. Washington, DTMB, February 1957. (DTMB Hydrodynamics Research and Development Report C-807), CONFIDENTIAL.

INITIAL DISTRIBUTION

9 Chief, Bureau of Naval Weapons
    DIS-31 (1)
    R-12 (1)
    RAAD-3 (1)
    RRRE (1)
    RRRE-71 (1)
    RRSY (1)
    RU (1)
    RUTO (1)
    RUTO-32 (1)
6 Chief, Bureau of Ships
    Code 106 (1)
    Code 335 (1)
    Code 421 (2)
    Code 442 (1)
    Code 664 (1)
1 Chief, Bureau of Yards and Docks (Research Division)
1 Chief of Naval Operations
5 Chief of Naval Research
    Code 429 (1)
    Code 438 (3)
    Code 466 (1)
8 David W. Taylor Model Basin
    Code 142 (1)
    Code 500 (1)
    Code 513 (1)
    Code 523B (1)
    Code 526 (1)
    Code 580 (1)
    Code 800 (1)
1 Naval Academy, Annapolis (Librarian)
1 Naval Civil Engineering Laboratory, Port Hueneme (Code L54)
1 Naval Engineering Experiment Station, Annapolis
2 Naval Ordnance Laboratory, White Oak
    Library Division, Desk HL (1)
1 Naval Postgraduate School, Monterey (Library, Technical Reports Section)
1 Naval Research Laboratory
1 Naval Torpedo Station, Keyport (Quality Evaluation Laboratory, Technical Library)
1 Naval Underwater Ordnance Station, Newport
2 Naval Weapons Plant (Code 752)
1 Navy Electronics Laboratory, San Diego

1 Navy Underwater Sound Laboratory, Fort Trumbull
1 Office of Naval Research Branch Office, Boston
1 Office of Naval Research Branch Office, Chicago
1 Office of Naval Research Branch Office, London
1 Office of Naval Research Branch Office, New York
1 Office of Naval Research Branch Office, Pasadena
1 Office of Naval Research Branch Office, San Francisco
1 Office of Ordnance Research, Durham
1 Waterways Experiment Station, Vicksburg
1 Air Force Office of Scientific Research (Mechanics Division)
1 Air Research and Development Command, Andrews Air Force Base
10 Armed Services Technical Information Agency (TIPCR)
1 Director of Defense (R & E) (Office of Fuels, Materials and
   Ordnance, Byard Belyea)
1 Committee on Undersea Warfare
1 Langley Research Center (John Parkinson)
1 Maritime Administration (Coordinator for Research)
1 Merchant Marine Academy, Kings Point, N. Y. (Head, Department
   of Engineering)
6 National Aeronautics and Space Administration
1 National Bureau of Standards (Fluid Mechanics Section,
   Dr. G. Schubauer)
2 National Science Foundation
      Director (1)
      Director, Engineering Sciences Division (1)
1 Office of Technical Services
5 British Joint Services Mission (Navy Staff), via BuWeps (DSC)
2 Defence Research Member, Canadian Joint Staff (W), via
   BuWeps (DSC)
1 Aerojet-General Corporation, Azusa, Calif. (C. A. Gongwer), via
   BuWepsRep
1 Aeronutronics, Newport Beach, Calif. (Ralph E. Smith)
1 Alden Hydraulic Laboratory, Worcester Polytechnic Institute,
   Worcester, Mass.
1 Applied Physics Laboratory, University of Washington, Seattle
1 AVCO Research Laboratory, Everett, Mass. (Technical Library)
1 Baker Manufacturing Company, Evansville, Wisc.
1 Bell Aerosystems Company, Buffalo (Technical Library)
1 Bendix Aviation Corporation, Pacific Division, North Hollywood
1 Boeing Airplane Company, Aero-Space Division, Seattle (Library,
   Organization No. 2-5190)
3 California Institute of Technology, Pasadena (Engineering Division)
      Dr. A. J. Acosta (1)
      Dr. M. S. Plesset (1)
      Dr. T. Y. Wu (1)
1 Chance Vought Aircraft, Inc., Dallas (Engineering Library)
1 Cleveland Pneumatics Industries, Inc., El Segundo, Calif. (Advanced
   Systems Development Division)
1 Clevite Research Center, Cleveland
1 CONVAIR Hydrodynamics Laboratory, San Diego

1 CONVAIR Scientific Research Laboratory, San Diego (A. L. Berlad)
1 Cornell University, Graduate School of Aeronautical Engineering, Ithaca (Prof. W. R. Sears)
2 Davidson Laboratory, Stevens Institute of Technology, Hoboken, N. J.
    A. Suarez (1)
    Dr. J. Breslin (1)
1 Douglas Aircraft Company, Inc., El Segundo, Calif. (Aerodynamics Section, A. M. O. Smith)
1 Eastern Research Group, New York City (Dr. L. Meyerhoff)
1 EDO Corporation, College Point, N. Y. (S. Fenn)
1 Electric Boat Division, General Dynamics Corporation, Groton, Conn.
1 Engineering Societies Library, New York City
1 General Electric Company, Defense Electronics Division, Pittsfield, Mass. (Engineering Librarian)
1 General Electric Company, Schenectady (Librarian, LMEE Department)
1 Gibbs and Cox, Inc., New York City (Dr. S. Hoerner)
1 Grumman Aircraft Engineering Corporation, Bethpage, N. Y. (Chief of Preliminary Design)
1 Grumman Aircraft Engineering Corporation, Dynamics Development Division, Babylon, N. Y.
1 Hudson Laboratories, Columbia University, Dobbs Ferry, N. Y.
1 Hughes Aircraft Company, Culver City, Calif.
2 Hydrodynamics Laboratory, CIT, Pasadena
    Dr. V. A. Vanoni (1)
    T. Kiceniuk (1)
1 Hydronautics, Inc., Rockville, Md.
1 Lockheed Aircraft Corporation, Burbank, Calif.
1 Lockheed Aircraft Corporation, Missiles and Space Division, Palo Alto, Calif. (R. W. Kermeen)
2 Massachusetts Institute of Technology, Cambridge
    Department of Naval Architecture and Marine Engineering
      Prof. L. Troost (1)
      Prof. M. Abkowitz (1)
1 McDonnell Aircraft Corporation, St. Louis
1 Miami Shipbuilding Corporation, Miami (P. Buhlar)
1 New York State Maritime College, Fort Schuyler (Librarian)
1 North American Aviation, Inc., Los Angeles (Technical Library, Department 56)
1 Operations Research, Inc., Los Angeles (Sidney Thurston)
3 Ordnance Research Laboratory, Pennsylvania State University, University Park
    Dr. B. W. McCormick (1)
    Dr. G. F. Wislicenus (1)
    Development Contract Administrator (1)
1 Pacific Aeronautical Library of the IAS, Los Angeles
1 Philco Corporation, Philadelphia (Engineering Library) via RInsMat
1 Polytechnic Institute of Brooklyn (Department of Aeronautical Engineering and Applied Mechanics, Prof. A. Ferri)

ABSTRACT CARD

U. S. Naval Ordnance Test Station
Studies of a Ventilated Supercavitating Propeller
on a Torpedo Test Vehicle. Part 1. Performance
Results, by Paul C. Roberts. China Lake, Calif.,
NOTS, 21 February 1961. 32 pp. (NAVWEPS Re-
port 7628, Part 1, NOTS TP 2633), UNCLASSIFIED.
ABSTRACT. A torpedo test vehicle utilizing a
ventilated supercavitating propeller was the subject
of an experimental program carried out on the
underwater cableway facility at Morris Dam.

(Over)
1 card, 4 copies

U. S. Naval Ordnance Test Station
Studies of a Ventilated Supercavitating Propeller
on a Torpedo Test Vehicle. Part 1. Performance
Results, by Paul C. Roberts. China Lake, Calif.,
NOTS, 21 February 1961. 32 pp. (NAVWEPS Re-
port 7628, Part 1, NOTS TP 2633), UNCLASSIFIED.
ABSTRACT. A torpedo test vehicle utilizing a
ventilated supercavitating propeller was the subject
of an experimental program carried out on the
underwater cableway facility at Morris Dam.

(Over)
1 card, 4 copies

U. S. Naval Ordnance Test Station
Studies of a Ventilated Supercavitating Propeller
on a Torpedo Test Vehicle. Part 1. Performance
Results, by Paul C. Roberts. China Lake, Calif.,
NOTS, 21 February 1961. 32 pp. (NAVWEPS Re-
port 7628, Part 1, NOTS TP 2633), UNCLASSIFIED.
ABSTRACT. A torpedo test vehicle utilizing a
ventilated supercavitating propeller was the subject
of an experimental program carried out on the
underwater cableway facility at Morris Dam.

(Over)
1 card, 4 copies

U. S. Naval Ordnance Test Station
Studies of a Ventilated Supercavitating Propeller
on a Torpedo Test Vehicle. Part 1. Performance
Results, by Paul C. Roberts. China Lake, Calif.,
NOTS, 21 February 1961. 32 pp. (NAVWEPS Re-
port 7628, Part 1, NOTS TP 2633), UNCLASSIFIED.
ABSTRACT. A torpedo test vehicle utilizing a
ventilated supercavitating propeller was the subject
of an experimental program carried out on the
underwater cableway facility at Morris Dam.

(Over)
1 card, 4 copies

NAVWEPS Report 7628
Part 1

Vehicle runs, incorporating an 11-inch-diameter ventilated supercavitating propeller (DTMB 3819), showed the propulsive efficiency to average 79%. As gas was passed through the blade-ventilation holes in increasing amounts, the advance ratio progressively decreased by 10% but it could not be concluded that the efficiency was directly affected. Propeller performance data obtained with the actual test torpedo agreed with water-tunnel results reported by other laboratories.